PHYSICS AND CHEMISTRY OF SOLID STATE
V. 22, No. 4 (2021) pp. 761-766
Section: Technology

DOI: 10.15330/pcss.22.4.761-766

Vasyl Stefanyk Precarpathian National University

ФІЗИКА І ХІМІЯ ТВЕРДОГО ТІЛА
Т. 22, № 4 (2021) С. 761-766
Технічні науки

UDK: 546.882 ISSN 1729-4428

L. Romaka[1], V.V. Romaka[2], Yu. Stadnyk[1], V. Pashkevych[3]

Phase equilibrium diagram of the Hf-Fe-Sn system at 1070 K

[1]*Inorganic Chemistry Department, Ivan Franko L'viv National University,Kyryla and Mefodiya str. 6, 79005 L'viv, Ukraine*
[2]*Techniscne Universitat Dresden, Bergstrasse 66, 01069 Dresden, Germany*
[3]*Lviv Polytechnic National University, S. Bandera Str. 12, 79013, Lviv, Ukraine, lyubov.romaka@gmail.com*

Experimental studies of the phase equilibrium diagram of the Hf-Fe-Sn ternary system at 1070 K were performed by X-ray powder diffractometry, scanning electron microscopy and electron probe microanalysis techniques in the whole concentration range. At annealing temperature four ternary compounds are realized: Hf_6FeSn_2 (K_2UF_6 structure type, space group *P*-62*m*), $Hf_{1.8}Fe_5Sn_{3.8}$ ($Hf_{1.82}Fe_5Sn_{3.82}$ structure type, space group *Cmmm*), $Hf_3Fe_4Sn_4$ ($Zr_3Fe_4Sn_4$ structure type, space group *Pnma*), and $Hf_9Fe_{3.7}Sn_{10.3}$ ($Hf_9Fe_4Sn_{10}$ structure type, space group $Cmc2_1$). An existence of the $Hf_{1-x}Fe_{2+x-y}Sn_y$ solid solution formed by substitution of the iron atoms by tin in the $Hf_{1-x}Fe_{2+x}$ ($MgZn_2$-type) binary compound up to 19 at. % Sn was found. Solubility of Fe in the Hf_5Sn_3 binary (Mn_5Si_3-type) extends up to 10 at. % (a=0.8363(2)-0.8324(4), c=0.5726(1)-0.5686(4) nm).

Keywords: Intermetallics; Phase diagrams; X-ray diffraction; Scanning electron microscopy.

Received 9 July 2021; Accepted 15 November 2021.

Introduction

Hafnium-based alloys are employed in different industrial fields (nuclear reactor, medicine, microprocessors, etc.). Some intermetallic compounds of Hf and the transition metals Fe, Co, Pd and Pt have been investigated as hydrogen-storage materials because of their capability to form hydrides with high hydrogen to metal ratios at room temperature [1]. Influence of Hf impurity on microstructure and mechanical properties of the W-Fe-Ni alloys was reported in Ref. [2]. Doping of the TiFe phase by hafnium has a positive effect on the activation properties [3].

Despite the increasing importance of hafnium in numerous technological applications, experimental and computational data on its alloys is sparse. These computations predict novel unsuspected compounds and indicate that some reported compounds may actually be unstable at low temperatures [4].

Among ternary intermetallics half-Heusler phases HfNiSn, HfCoSb, HfRhSb, HfPtSb (MgAgAs-type) exhibit semiconducting behavior [5-7] and represent basis for creation of the new thermoelectric materials.

The investigation of the metallic systems at selected temperatures is important step to provide valuable information of the sample preparation method, temperature of the heat treatment, stability, composition and crystal structure peculiarity of the ternary compounds. This knowledge play significant role for studies of the physical property which in many cases are strongly dependent on the synthesis, heat treatments, stability, homogeneity domains, and structural disordering of the intermediate phases. At present among metallic systems Hf-M-Sn (M-*d*-element) the phase equilibrium diagrams were studied for the Hf-Ni-Sn [8], Hf-Co-Sn [9] and Hf-Ag-Sn [10] ternary systems. For Hf-containing systems with other *d*-element the structural and physical characteristics of individual compounds have been studied only [11]. Investigated phase diagrams of the Hf-{Co,Ni,Ag}-Sn systems demonstrate an influence of *d*-metals on the interaction of Hf and Sn with Ni, Co or Ag. Among them only in the Hf-Ag-Sn system at 770 K no ternary phases were observed. Both Hf-Ni-Sn and Hf-Co-Sn systems are characterized by the presence of isotypic HfM_2Sn ($MnCu_2Al$-type) and Hf_6M_2Sn (K_2UF_6-type) [8, 9, 12] compounds. In the case of equiatomic compounds the type of 3*d*-metal leads to the different crystal structure of

the HfMSn stannides – cubic MgAgAs-type for Hf(Ni,Pd,Pt)Sn, hexagonal ZrNiAl-type for Hf(Co,Rh,Ir)Sn, and hexagonal LiGaGe-type for HfCuSn [11, 13,14].

To know the intrinsic properties of the intermetallics the first step is to determine their relations with other phases and to evaluate the compositions and homogeneity range. The subject of the present paper consists of the complete investigation of the Hf-Fe-Sn phase equilibrium diagram at 1070 K by X-ray powder diffractometry and electron probe microanalysis (EPMA).

I. Methods and materials

For our investigations samples were synthesized by an arc-melting method under purified (Ti as a getter) Ar-protected atmosphere using the starting metals with a purity: Hf – 99.98 wt. %; Fe - 99.99 wt.%; and Sn-99.99 wt.%. In order to ensure the homogeneity the arc-melted buttons were turned over and re-melted with weight losses lower than 1 %. Taking into account high melting temperature of Hf and Fe the alloys were annealed at 1070 K (temperature control ±2 K) during four weeks in evacuated quartz ampoules, and then quenched in cold water without breaking of the ampoules.

Prepared samples were tested by X-ray powder diffraction (DRON-4.0 diffractometer, FeKα radiation) to obtain an information on their phase composition and formed intermediate phases (PowderCell program [15]).

The chemical and phase compositions of the prepared samples were examined by Scanning Electron Microscopy (SEM) using Carl Zeiss DSM 962 and Tescan Vega 3 LMU electron microscopes with a Link EDX system operated at 20 kV and 60 μA. Quantitative electron probe microanalysis (EPMA) of the alloys was carried out using an energy-dispersive X-ray analyzer with the pure elements as standards (*K*- and *L*-lines were used). Crystallographic parameters were calculated using WinCSD program package [16].

II. Results and discussion

To establish the phase relations in the Hf-Fe-Sn system the prepared alloys were examined by X-ray phase analysis and scanning electron microscopy. Phase compositions of the selected alloys at 1070 K are presented in Table 1. The SEM-pictures of some alloys are shown in Figs. 1, 2. Based on the obtained results isothermal section of the Hf-Fe-Sn system was constructed and illustrated in Fig. 3.

Data on the phase diagrams of the Hf−Fe, Hf−Sn, and Fe−Sn binary systems, which limit the studied ternary Hf-Fe-Sn system, and the structural data of the corresponding binary compounds were used from Refs. [17-19]. Under used in our work conditions the presence of almost all binary compounds in the Hf-Sn, Fe-Sn and Hf-Fe systems corresponded to the reference data was confirmed. In the Fe-Sn system the Fe_3Sn_2 (Fe_3Sn_2-type), $Fe_{1.67}Sn$ (Ni_2In-type) and Fe_3Sn (Mg_3Cd-type) binaries were identified. In the Hf-Sn system the Hf_5Sn_3 (Mn_5Si_3-type), Hf_5Sn_4 (Ti_5Ga_4-type) and $HfSn_2$ ($CrSi_2$-type) compounds have been confirmed at 1070 K, while a formation of the HfSn (FeSi-type) binary was not detected under our conditions. Sample $Hf_{50}Sn_{50}$ contains Hf_5Sn_4 and $HfSn_2$ phases in equilibrium.

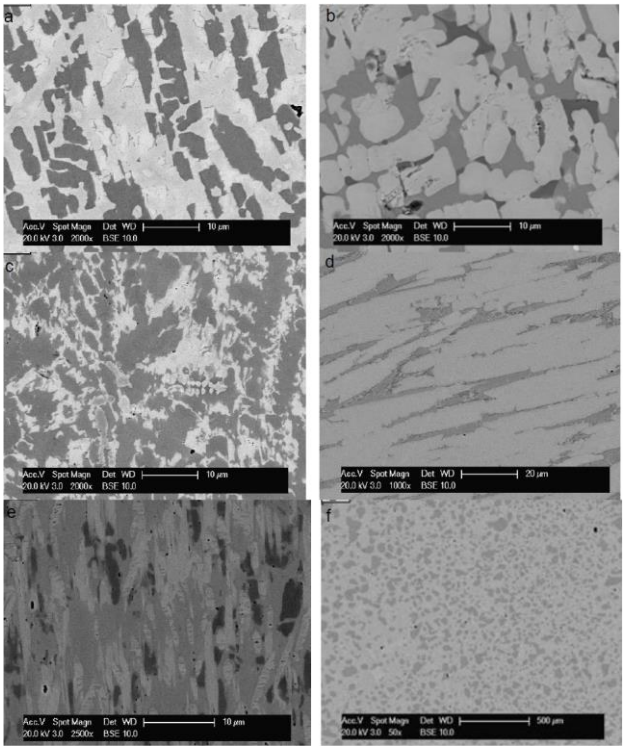

Fig. 1. Electron microphotographs of the alloys: a) $Hf_{50}Fe_{45}Sn_5$ – Hf_2Fe (grey phase), Hf_6FeSn_2 (white phase), $HfFe_2$ (black phase); b) $Hf_{15}Fe_{70}Sn_{15}$ - $Hf_{1-x}Fe_{2+x-y}Sn_y$ (white phase), Fe_3Sn (grey phase), Fe (black phase); c) $Hf_{40}Fe_{40}Sn_{20}$ – $Hf_5Fe_xSn_{3-x}$ (white phase), $Hf_{1-x}Fe_{2+x-y}Sn_y$ (grey dark phase), Hf_5Sn_4 (grey light phase); d) $Hf_{60}Fe_{10}Sn_{30}$ - $Hf_5Fe_xSn_{3-x}$ (grey light phase), $Hf_{1-x}Fe_{2+x-y}Sn_y$ (grey dark phase); e) $Hf_{45}Fe_{15}Sn_{40}$ - $Hf_9Fe_{3.7}Sn_{10.3}$ (grey phase), Hf_5Sn_4 (grey light phase), $Hf_{1-x}Fe_{2+x-y}Sn_y$ (black phase); f) $Hf_8Fe_{46}Sn_{46}$ – Fe_3Sn_2 (dark grey phase), $Hf_{1.8}Fe_5Sn_{3.8}$ (grey phase), Sn (light phase).

Analysis of the binary samples of the Hf-Fe system confirmed the presence of the $HfFe_2$ and Hf_2Fe (Ti_2Ni-type) compounds. Two polymorphic forms were identified for $HfFe_2$ phase – hexagonal modification with $MgZn_2$-type and cubic one with $MgCu_2$-type [17]. Hexagonal modification $Hf_{1-x}Fe_{2+x}$ ($MgZn_2$-type) binary is characterized by large homogeneity range limited from EPMA data by $Hf_{25.44}Fe_{74.56}$ and $Hf_{33.63}Fe_{66.37}$ compositions. Determined from EPMA data composition for $HfFe_2$ cubic modification is $Hf_{37.24}Fe_{62.76}$.

According to performed XRPD and EPM analyses in the Hf-Fe-Sn system at 1070 K four ternary compounds were confirmed (Fig. 3). Crystallographic characteristics of the observed ternary compounds are given in Table 2. $Hf_3Fe_4Sn_4$ and Hf_6FeSn_2 compounds form at corresponding stoichiometry. The compositions of the $Hf_{1.8}Fe_5Sn_{3.8}$ [20] ($Hf_{17.18}Fe_{46.95}Sn_{35.87}$) and $Hf_9Fe_{3.7}Sn_{10.3}$ [21] ($Hf_{39.70}Fe_{15.88}Sn_{44.42}$) compounds were confirmed by EPMA data.

Table 1

Phase composition and EPMA data for selected alloys in the Hf-Fe-Sn system

Nominal composition	Phase	Structure type	Lattice parameters, nm			EPMA data, at %		
			a	*b*	*c*	Hf	Fe	Sn
$Hf_{50}Fe_{45}Sn_5$	Hf_6FeSn_2	K_2UF_6	0.7762(8)		0.3378(5)	67.16	12.92	19.92
	Hf_2Fe	Ti_2Ni	1.2007(3)			66.37	32.98	0.65
	$HfFe_2$	$MgCu_2$	0.7048(8)			37.01	65.54	0.45
$Hf_{35}Fe_{55}Sn_{10}$	$HfFe_2$	$MgZn_2$	0.4942(6)		0.8157(7)			
	Hf_6FeSn_2	K_2UF_6	not determined					
$Hf_{15}Fe_{70}Sn_{15}$	$HfFe_2$	$MgZn_2$	0.4937(2)		0.8011(5)	25.44	66.88	7.68
	Fe_3Sn	Mg_3Cd	0.5422(6)		0.4318(6)	1.06	74.18	24.76
	(Fe)	W	0.2884(2)				100.0	
$Hf_{70}Fe_{10}Sn_{20}$	Hf_6FeSn_2	K_2UF_6	0.7801(2)		0.3426(2)			
	(Hf)	Mg	0.3187(1)		0.5092(2)			
	Hf_5Sn_3	Mn_5Si_3	0.8328(9)		0.5764(9)			
$Hf_{72}Fe_{14}Sn_{14}$	Hf_6FeSn_2	K_2UF_6	0.7791(2)		0.3427(2)			
	Hf_2Fe	Ti_2Ni	1.2011(4)					
	(Hf)	Mg	0.3188(3)		0.5090(2)			
$Hf_{25}Fe_{50}Sn_{25}$	$HfFe_2$	$MgZn_2$	0.5096(3)		0.8276(5)	24.72	57.10	18.18
	$Hf_3Fe_4Sn_4$	$Zr_3Fe_4Sn_4$	0.8126(3)	0.8882(4)	1.0602(5)	27.98	36.21	35.81
	$Hf_{1.8}Fe_5Sn_{3.8}$	$Hf_{1.8}Fe_5Sn_{3.8}$	0.9702(4)	1.6823(6)	0.8446(3)	17.18	46.95	35.87
$Hf_{50}Fe_{25}Sn_{25}$	$Hf_5Sn_{3-x}Fe_x$	Mn_5Si_3	0.8363(8)		0.5720(5)			
	$HfFe_2$	$MgZn_2$	not determined					
$Hf_{10}Fe_{55}Sn_{35}$	$Hf_{1.8}Fe_5Sn_{3.8}$	$Hf_{1.8}Fe_5Sn_{3.8}$	0.9704(4)	1.6822(7)	0.8446(3)			
	$Fe_{1.67}Sn$	Ni_2In	0.4218(3)		0.5211(3)			
$Hf_{56}Fe_{11}Sn_{33}$	$Hf_5Sn_{3-x}Fe_x$	Mn_5Si_3	0.8320(7)		0.5684(4)			
	$Hf_{1-x}Fe_{2+x-y}Sn_y$	$MgZn_2$	0.5093(2)		0.8276(5)			
	Hf_5Sn_4	Ti_5Ga_4	0.8683(4)		0.7597(4)			
$Hf_{10}Fe_{60}Sn_{30}$	$Hf_{1.8}Fe_5Sn_{3.8}$	$Hf_{1.8}Fe_5Sn_{3.8}$	0.9703(5)	1.6824(6)	0.8446(3)	17.54	46.43	36.03
	Fe_3Sn	Mg_3Cd	0.5462(3)		0.4365(4)		74.87	25.13
$Hf_{30}Fe_{40}Sn_{30}$	$Hf_3Fe_4Sn_4$	$Zr_3Fe_4Sn_4$	0.8126(3)	0.8884(3)	1.0602(6)			
	$HfFe_2$	$MgZn_2$	0.5093(3)		0.8274(5)			
	$Hf_9Fe_{3.7}Sn_{10.3}$	$Hf_9Fe_{3.7}Sn_{10.3}$	0.5676(5)	3.5875(7)	0.8873(5)			
$Hf_{20}Fe_{45}Sn_{35}$	$Hf_3Fe_4Sn_4$	$Zr_3Fe_4Sn_4$	0.8126(3)	0.8884(2)	1.0601(5)			
	$Hf_{1.8}Fe_5Sn_{3.8}$	$Hf_{1.8}Fe_5Sn_{3.8}$	0.9704(4)	1.6820(7)	0.8445(4)			
$Hf_{45}Fe_{15}Sn_{40}$	$Hf_9Fe_{3.7}Sn_{10.3}$	$Hf_9Fe_{3.7}Sn_{10.3}$	0.5677(7)	3.5875(5)	0.8875(4)	40.03	16.79	43.18
	Hf_5Sn_4	Ti_5Ga_4	0.8684(3)		0.7597(3)	56.44		43.56
	$HfFe_{2-x}Sn_x$	$MgZn_2$	0.5095(4)		0.8273(5)	35.64	45.78	18.58
$Hf_{20}Fe_{40}Sn_{40}$	$Hf_3Fe_4Sn_4$	$Zr_3Fe_4Sn_4$	0.8128(3)	0.8885(3)	1.0662(4)	29.00	35.68	35.32
	(Sn)	Sn	0.5828(4)		0.3177(2)			100.0
	$Hf_{1.8}Fe_5Sn_{3.8}$	$Hf_{1.8}Fe_5Sn_{3.8}$	0.9705(5)	1.6822(6)	0.8444(5)	17.99	47.19	34.82
$Hf_8Fe_{46}Sn_{46}$	Fe_3Sn_2	Fe_3Sn_2	0.5365(3)		1.9724(5)		59.62	40.38
	$Hf_{1.8}Fe_5Sn_{3.8}$	$Hf_{1.8}Fe_5Sn_{3.8}$	0.9705(5)	1.6821(7)	0.8446(5)	17.20	47.03	35.77
	(Sn)	Sn	0.5799(2)		0.3177(3)			100.0
$Hf_{25}Fe_{25}Sn_{50}$	$Hf_3Fe_4Sn_4$	$Zr_3Fe_4Sn_4$	0.8130(2)	0.8885(2)	1.0661(3)	29.28	34.75	35.97
	(Sn)	Sn	0.5828(2)		0.3178(2)			100.0
	$Hf_9Fe_{3.7}Sn_{10.3}$	$Hf_9Fe_{3.7}Sn_{10.3}$	0.5676(5)	3.5875(7)	0.8874(3)	39.28	17.57	43.15
$Hf_{40}Fe_{10}Sn_{50}$	$HfSn_2$	$CrSi_2$	0.5470(2)		0.7595(4)	33.65	1.91	64.44
	$Hf_9Fe_{3.7}Sn_{10.3}$	$Hf_9Fe_{3.7}Sn_{10.3}$	0.5675(6)	3.5876(7)	0.8875(4)	40.89	17.00	42.11
	Hf_5Sn_4	Ti_5Ga_4	0.8692(3)		0.5869(3)	54.20		45.80
$Hf_{30}Fe_{10}Sn_{60}$	(Sn)	Sn	0.5829(4)		0.3181(3)			
	$HfSn_2$	$CrSi_2$	0.5469(3)		0.7596(4)			
	$Hf_9Fe_{3.7}Sn_{10.3}$	$Hf_9Fe_{3.7}Sn_{10.3}$	0.5675(6)	3.5876(7)	0.8874(5)			

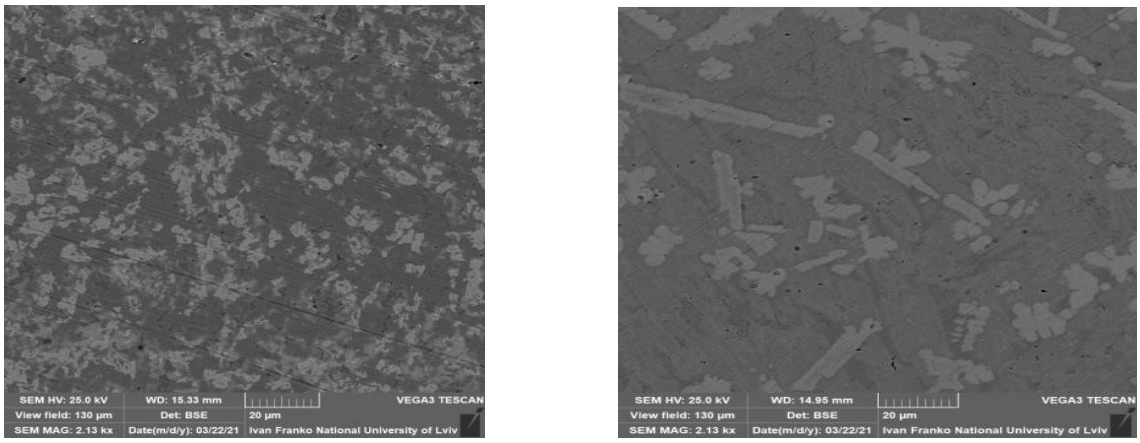

a b

Fig. 2. Electron microphotographs of the alloys: a) $Hf_{20}Fe_{45}Sn_{35}$ - $Hf_{1.8}Fe_5Sn_{3.8}$ (grey phase), $Hf_3Fe_4Sn_4$ (light phase); b) $Hf_{67}Fe_{18}Sn_{15}$ – Hf_6FeSn_2 (grey phase), Hf (light phase), Hf_2Fe (dark grey phase)

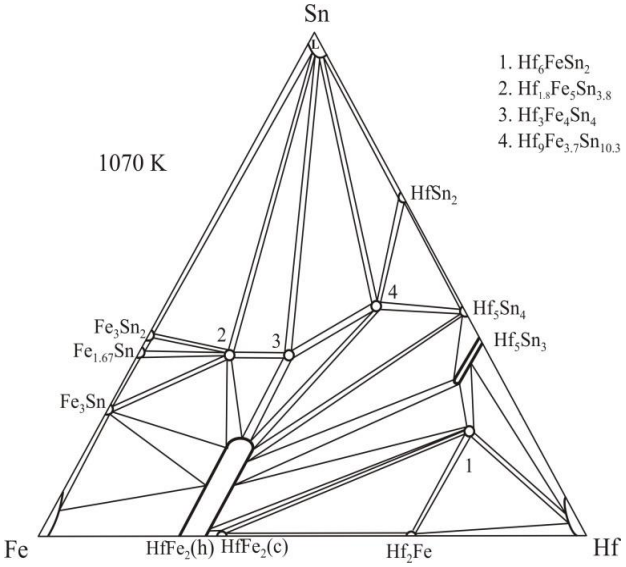

Fig. 3. Isothermal section of the Hf-Fe-Sn phase diagram at 1070 K.

In Ref. [22] the authors studied the $M'_6M''_{1.5+x}Sn_{1.5-x}$ compounds (M'=Zr, Hf, M''-d-metal) with K_2UF_6 type structure. In this work $Hf_6Fe_{1.5+x}Sn_{1.5-x}$ compound was reported as isotypic with $Zr_6Co_{1.65}Sn_{1.35}$ stannide with lattice parameters a=0.7909, c=0.3424 nm. In our work we confirmed this compound, but the determined composition $Hf_{67.16}Fe_{11.92}Sn_{20.92}$ from EPMA data differ from composition reported in [22] ($Hf_{67}Fe_{18}Sn_{15}$) and rather corresponds to the stoichiometry Hf_6FeSn_2. In this case crystallographic position 2*d* is occupied exclusively by Sn atoms. Analysis of the $Hf_{67}Fe_{18}Sn_{15}$ sample showed that it is located in the three-phase field and contains Hf_6FeSn_2, Hf_2Fe and Hf in equilibrium (Fig. 2b).

We also checked the possible formation of the $HfFe_6Sn_6$ compound similarly to the related Zr-Fe-Sn system [23]. According to the phase analysis of the annealed at 1070 K and as-cast sample compound with stoichiometry 1:6:6 was not observed in the Hf-Fe-Sn system. Examined sample $Hf_8Fe_{46}Sn_{46}$ (1070 K) belongs to three-phase field and contains $Hf_{1.8}Fe_5Sn_{3.8}$, Fe_3Sn_2 and Sn in equilibrium (Fig. 1f).

With regards the literature data in the systems with two *d*-elements and tin the ternary phases with Hf_5CuSn_3-type are formed. In the previously studied Hf–{Co, Ni, Ag}–Sn systems [8-10] the formation of the $Hf_5M_xSn_3$ solid solutions was revealed, and the limiting compositions of these solid solutions at x = 1.0 were considered as ternary phases with Hf_5CuSn_3-type. To check the formation of analogous solid solution in the Hf-Fe-Sn system the region along "Hf_5FeSn_3"-Hf_5Sn_3 line was studied. The XRPD and EPM analyses of the corresponding samples indicated the formation of the substitution-type solid solution $Hf_5Fe_xSn_{3-x}$ along isoconcentrate 62.5 at. % of Hf up to Fe content ~10 at. %. (Table 3). Decreasing of the volume cell with Fe content confirmed the substitution of the Sn atoms (r_{Sn}=0.158 nm) by smaller Fe atoms (r_{Fe}=0.127 nm). The $Hf_{56}Cu_{11}Sn_{33}$ alloy is located in the three-phase field and contains $Hf_5Fe_xSn_{3-x}$, $Hf_{1-x}Fe_{2+x-y}Sn_y$ and Hf_5Sn_4 phases.

The formation of the substitution-type solid solution $Hf_{1-x}Fe_{2+x-y}Sn_y$ was established on the basis of the $Hf_{1-x}Fe_{2+x}$ binary compound with $MgZn_2$-type. Solubility of Sn along isoconcentrates of Hf reaches up to about 19 at. %. Composition and lattice parameters of the samples of the $Hf_{1-x}Fe_{2+x-y}Sn_y$ solid solution along isoconcentrate 30 at. % of Hf are presented in Table 4. The limit

Table 2.

Crystallographic characteristics of the ternary compounds in the Hf-Fe-Sn system

N*	Compound	Structure type	Space group	Lattice parameters, nm		
				a	*b*	*c*
1	Hf_6FeSn_2	K_2UF_6	*P*-62*m*	0.7901(2)		0.3426(2)
2	$Hf_{1.8}Fe_5Sn_{3.8}$	$Hf_{1.82}Fe_5Sn_{3.82}$	*Cmmm*	0.9689(7)	1.6842(4)	0.8448(6)
3	$Hf_3Fe_4Sn_4$	$Zr_3Fe_4Sn_4$	*Pnma*	0.8130(2)	0.8885(2)	1.0661(3)
4	$Hf_9Fe_{3.7}Sn_{10.3}$	$Hf_9Fe_4Sn_{10}$	*Cmc*2_1	0.5678(3)	3.4952(6)	0.8877(4)

*Compound number corresponds to Fig. 1.

Table 3
Composition and lattice parameters of the samples of the $Hf_5Sn_{3-x}Fe_x$ solid solution

Composition	Lattice parameters, nm		V, nm^3
	a	*c*	
$Hf_{62.5}Sn_{37.5}$ (Hf_5Sn_3)	0.8363(2)	0.5726(2)	0.3403
$Hf_{62.5}Fe_3Sn_{34.5}$	0.8351(2)	0.5696(4)	0.3386
$Hf_{62.5}Fe_5Sn_{32.5}$	0.8335(2)	0.5694(1)	0.3393
$Hf_{62.5}Fe_7Sn_{30.5}$	0.8330(1)	0.5690(3)	0.3376
$Hf_{62.5}Fe_{10}Sn_{27.5}$	0.8324(4)	0.5686(4)	0.3376
$Hf_{62.5}Fe_{12}Sn_{25.5}$	0.8318(4)	0.5683(3)	0.3375

Table 4
Composition and lattice parameters of the samples of the $Hf_{1-x}Fe_{2+x-y}Sn_y$ solid solution

Composition	Lattice parameters, nm		V, nm^3
	a	*c*	
$Hf_{30}Fe_{70}$	0.4947(2)	0.8054(5)	0.1706
$Hf_{30}Fe_{67}Sn_3$	0.4950(2)	0.8066(6)	0.1711
$Hf_{30}Fe_{65}Sn_5$	0.4964(1)	0.8085(6)	0.1725
$Hf_{30}Fe_{62.5}Sn_{7.5}$	0.4973(2)	0.8087(7)	0.1732
$Hf_{30}Fe_{60}Sn_{10}$	0.4978(2)	0.8088(7)	0.1736
$Hf_{30}Fe_{57.5}Sn_{12.5}$	0.5068(8)	0.8231(6)	0.1830
$Hf_{30}Fe_{55}Sn_{15}$	0.5092(6)	0.8261(7)	0.1855
$Hf_{30}Fe_{52}Sn_{18}$	0.5095(2)	0.8277(5)	0.1861
$^*Hf_{30}Fe_{50}Sn_{20}$	0.5094(3)	0.8277(7)	0.1860

* - two phase sample.

composition of this solid solution was estimated from the systematic analysis of the cell parameters and by the results of electron probe microanalysis. Sample $Hf_{40}Fe_{40}Sn_{20}$ is located in the three-phase field and contains $Hf_{1-x}Fe_{2+x-y}Sn_y$ ($Hf_{33.07}Fe_{48.28}Sn_{18.65}$), $Hf_5Fe_xSn_{3-x}$ and Hf_5Sn_4 phases in equilibrium (Fig. 1, c).
The solubility of the third components in other binary compounds is less than 1-1.5 at. %.

III. Final remarks

Performed in our work studies showed that interaction of hafnium with iron and tin at 1070 K results in formation of four ternary compounds Hf_6FeSn_2, $Hf_{1.8}Fe_5Sn_{3.8}$, $Hf_3Fe_4Sn_4$ and $Hf_9Fe_{3.7}Sn_{10.3}$ and prolonged $Hf_{1-x}Fe_{2+x-y}Sn_y$ and $Hf_5Fe_xSn_{3-x}$ solid solutions. Comparing the studied Hf-Fe-Sn system and taking into account the literature data for the related systems Hf-{Co,Ni,Cu,Ag}-Sn we may note that the ternary compounds with equiatomic composition appear only in the systems with Co, Ni, and Cu. Depending on *d*-element they crystallize in different structure types [8, 9, 14]. The similarity in the interaction of the components in the investigated Hf-{Fe,Co,Ni}-Sn systems is displayed by the formation of the Hf_6MSn_2 compounds with K_2UF_6 structure type [22]. Other ternary phases, $Hf_{1.8}Fe_5Sn_{3.8}$, $Hf_3Fe_4Sn_4$ and $Hf_9Fe_{3.7}Sn_{10.3}$, are typical only for the Hf-Fe-Sn system.

Romaka Lyubov - Ph.D., Senior Scientist of Ivan Franko National University of Lviv;
Romaka Vitaliy - D.Sc., doctor of material science, Institute for Solid State Research, Dresden, Germany;
Stadnyk Yuriy - Ph.D., Senior Scientist of Ivan Franko National University of Lviv;
Pashkevych Volodymyr - docent of National University "Lvivska Politechnika".

[1] A. Baudry, P. Boyer, L.P. Ferreira, S. W. Harris, S. Miraglia, L. Pontonnier, J. Phys.: Condens. Matter. 4, 5025 (1992), https://doi.org/10.1088/0953-8984/4/21/018.
[2] T. Dewen, S. Zhou, Y. Liang, J. Alloys Compd. 724, 1176 (2017), https://doi.org/10.1016/j.jallcom.2017.07.037.
[3] V. Razafindramanana, S. Corsse, J. Huot, J.L. Bobet, Energies 12(18), 3477 (2019), https://doi.org/10.3390/en12183477.
[4] O. Levy, Gus L.W. Hart, S. Curtarolo, Acta Mater. 58, 2887 (2010), https://doi.org/10.1016/j.actamat.2010.01.017.
[5] F.G. Aliev, N.B. Brandt, V.V. Moshchalkov, V.V. Kozyrkov, R.V. Skolozdra, A.I. Belogorokhov, Z. Phys. B. Condens. Matter. 75(2), 167 (1989), https://doi.org/10.1007/BF01307996.
[6] W. Xie, A. Weidenkaff, X. Tang, Q. Zhang, J. Poon, T.M. Tritt, Nanomaterials 2, 379 (2012), https://doi.org/10.3390/nano2040379.
[7] M. Gürth, G. Rogl, V.V. Romaka, A. Grytsiv, E. Bauer, P. Rogl, Acta Mater. 104, 210 (2016), https://doi.org/10.1016/j.actamat.2015.11.022.
[8] Yu.V. Stadnyk, L.P. Romaka, J. Alloys Compd. 316, 169 (2001), https://doi.org/10.1016/S0925-8388(00)01036-7.
[9] L. Romaka, Yu.V. Stadnyk, O.I. Bodak, J. Alloys Compd. 317-318, 347 (2001), https://doi.org/10.1016/S0925-8388(00)01428-6.
[10] N. Melnychenko-Koblyuk, V.V. Romaka, L. Romaka, Yu. Stadnyk, Chem. Met. Alloys 4, 234 (2011).
[11] V.V. Romaka, L.P. Romaka, V.Ya. Krajovskyj, Yu.V. Stadnyk, Stannides of rare earth and transition metals, Lviv Polytech. Univ. 2015, 221 p.
[12] R.V. Skolozdra, Yu.V. Stadnyk, E.E. Starodynova, Ukr. Fiz. J. 32, 1258 (1986).
[13] A.E. Dwight, J. Less-Common Met. 34, 279 (1974), https://doi.org/10.1016/0022-5088(74)90170-2.
[14] R.V. Skolozdra, L.P. Romaka, L.G. Alselrud, G.A. Melnik, Ya.T. Tatomir, Neorg. Mater. 35(4), 1 (1999),

[15] W. Kraus, G. Nolze, POWDER CELL – a program for the representation and manipulation of crystal structures and calculation of the resulting X-ray powder patterns, J. Appl. Crystallogr. 29, 301 (1996), https://doi.org/10.1107/S0021889895014920.
[16] L. Akselrud, Yu. Grin, WinCSD: software package for crystallographic calculations (Version 4), J. Appl. Crystallogr. 47, 803 (2014), https://doi.org/10.1107/S1600576714001058.
[17] T.B. Massalski, in: Binary Alloy Phase Diagrams, ASM, Metals Park, Ohio, 1990.
[18] H. Okamoto, Desk Handbook: Phase Diagrams for Binary Alloys, (Materials Park (OH): American Society for Metals, 2000).
[19] K.H.J. Buschow, P.G. Van Engen, R. Jongebreur, J. Magn. Magn. Mater. 38, 1 (1983), https://doi.org/10.1016/0304-8853(83)90097-5.
[20] N.P. Calta, M.C. Francisco, C.D. Malliakas, J.A. Schlueter, M.G. Kanatsidis, Chem. Mater. 26, 6827 (2014), https://doi.org/10.1021/cm503466a.
[21] N.P. Calta, M.G. Kanatsidis, J. Solid State Chem. 236, 130 (2016), .https://doi.org/10.1016/j.jssc.2015.12.017.
[22] G.A. Melnyk, D. Fruchart, L.P. Romaka, Ju.V. Stadnyk, R.V. Skolozdra, J. Tobola, J. Alloys Compd. 267, L1 (1998), https://doi.org/10.1016/S0925-8388(97)00522-7.
[23] J.-C. Savidan, J.-M. Joubert, C. Toffolon-Masclet, Intermetallics 18, 2224 (2010), https://doi.org/10.1016/j.intermet.2010.07.007.

Л. Ромака[1], В.В. Ромака[2], Ю. Стадник[1], В. Пашкевич[3]

Діаграма фазових рівноваг системи Hf-Fe-Sn при 1070 K

[1]Львівський національний університет ім. І.Франка, вул. Кирила і Мефодія, 6, Львів, 79005, Україна,
[2]Технічний університет Дрезден, Бергштрассе, 66, 01069 Дрезден, Німеччина
[3]Національний університет "Львівська політехніка", вул. С. Бандери, 12, Львів, 79013, Україна,
lyubov.romaka@gmail.com

Експериментальне дослідження діаграми фазових рівноваг потрійної системи Hf-Fe-Sn виконано методами рентгенівської дифракції і скануючої електронної мікроскопії в повному концентраційному інтервалі при 1070 K. За температури дослідження в системі утворюються чотири тернарні сполуки: Hf_6FeSn_2 (структурний тип K_2UF_6, просторова група *P*-62*m*), $Hf_{1.8}Fe_5Sn_{3.8}$ (структурний тип $Hf_{1.82}Fe_5Sn_{3.82}$, просторова група *Cmmm*), $Hf_3Fe_4Sn_4$ (структурний тип $Zr_3Fe_4Sn_4$, просторова група *Pnma*) і $Hf_9Fe_{3.7}Sn_{10.3}$ (структурний тип $Hf_9Fe_4Sn_{10}$, просторова група *Cmc*2_1). На основі бінарної сполуки $Hf_{1-x}Fe_{2+x}$ (структурний тип $MgZn_2$) встановлено утворення твердого розчину заміщення $Hf_{1-x}Fe_{2+x-y}Sn_y$ до вмісту 19 ат. % Sn. Розчинність Fe в бінарній сполуці Hf_5Sn_3 (структурний тип Mn_5Si_3) сягає до 10 ат. % (*a*=0.8363(2)-0.8324(4), *c*=0.5726(1)-0.5686(4) нм).

Ключові слова: Інтерметаліди; Фазова діаграма; Рентгенівська дифракція; Скануюча електронна мікроскопія.